UCLA
COMPUTATIONAL AND APPLIED MATHEMATICS

Nonlinear Galerkin Based Model Reduction

David G. Kan

November 1998

CAM Report 98-49

Department of Mathematics
University of California, Los Angeles
Los Angeles, CA. 90095-1555

Nonlinear Galerkin Based Model Reduction

David G. Kan
UCLA Department of Mathematics

November 19, 1998

Abstract

The nonlinear Galerkin methods have been proposed as improvements over the standard Galerkin methods in fluid dynamics. I extend these ideas to a general model reduction context-one in which a general system of differential equations take the place of the partial differential equation. A new method which improves the approximation of transient phases is derived in a similar fashion and implemented. Accuracy of the methods are analyzed and rigorous error bounds are obtained and compared. The methods are then applied to various problems, including problems from fluid mechanics and material science.

1 Background

A major goal of scientific computing and numerical analysis is the efficient and accurate computation of solutions to complicated problems based on their mathematical formulation. One of these problems is the solution of very large systems of ordinary differential equations (ODE's) (e.g., in chemical reactions [18], [25], [26]). These various systems often depend on so many unknowns that current computational technology cannot handle the systems as posed. In many applications, however, a much smaller subset of variables is representative of the whole system. Thus there is the possibility to approximate the solution accurately with a smaller system. The process of identifying the representative variables and computing an approximate solution is called model reduction.

Model reduction is an established and important tool in control theory, Since control of a system often is more computationally intense than direct

simulation, special techniques for model reduction have been developed in this context. Several methods for reducing linear models were developed over the last two decades. Examples of these are balancing [24], continued fraction Padé methods [29] [27], techniques based on optimization [3], and singular perturbation [16]. Recently reduction of nonlinear models has been the subject of much study ([12], [17], [21], [22]).

A very important source of large ODE's systems is spatially discretized time dependent partial differential equations (PDE's). One example is the method of lines for which the first step is a finite difference or finite element approximation in space [4], [11], [20]. Another is the spectral method in which the first step is a Fourier or an orthogonal polynomial decomposition of the spatial variables [11], [28]. Lately wavelet spaces have also been used for the spatial representation [1]. After the spatial discretization, the resulting system of ODE's in practice is often very large.

In model reduction, there is the need for two steps:

1. Find representative variables as a subset of the original variables as a linear or nonlinear combination of the original variables.

2. Find an efficient way to use the information in the original system to calculate the evolution of the reduced system accurately.

Our research is concerning the second of these steps.

2 Basic Principles

2.1 General Techniques

In its most general form, model reduction attempts to simplify

$$\frac{dy}{dt} = f(y,t),\ y \in \mathbb{R}^d, \tag{2.1}$$

by finding a new set of unknowns $u \in \mathbb{R}^p$, $p < d$.

Here the new set of unknowns u a some linear or nonlinear function of y,

$$u = g(y,t). \tag{2.2}$$

The function g may be a simple projection, or a nonlinear function. In dynamical systems terms, these projecting functions produce a representation of the manifold in $\mathbb{R}^d$ containing the solution y or a representation of y

in the model reduced problem. This lower dimensional manifold often is an approximation of the global attractor of the solution operator of the system. The most naive of these approximations is a simple projection, e.g., onto low Fourier modes. The theory of inertial manifolds [5], [23] as computable approximations of the global attractor is the theoretical basis for the nonlinear Galerkin methods [19], which use nonlinear projecting functions.

So given such a g, time integration is performed to solve

$$\frac{du}{dt} = h(u,t), \tag{2.3}$$

where h describes the dynamics on the manifold. Then, after calculating, the original vector y can be recovered,

$$y \approx r(u,t), \tag{2.4}$$

in terms of u (see Method 5 below and [10]). Very often, however, not all of y is required but only some particular quantities $u = Ay$ where the vector u is of much lower dimension than y. This is common in control where u may even be a scalar.

2.2 Subset Reduction

We shall here consider the case where $u \in \mathbb{R}^p$ is given and a subset of $y \in \mathbb{R}^d$, $p < d$:

$$y = \begin{pmatrix} u \\ v \end{pmatrix}. \tag{2.5}$$

This corresponds to problem 2 in §1.

The vector u is then used as the unknowns for the system

$$\begin{cases} \frac{du}{dt} = f(u,v,t) \\ \frac{dv}{dt} = g(u,v,t), \end{cases} \tag{2.6}$$

in which the vector $(f,g)^T$ corresponds to the original f in (2.1).

Here we describe a few techniques in this context which are new or have been used in literature. The techniques reduce the number of differential equations, but may not, in this first step, reduce the number of unknowns.

Method 1: The standard Galerkin method (SGM) is the first example of such a technique. In the notation above, this method can be represented as:

$$\frac{d\tilde{u}}{dt} = f(\tilde{u}, 0, t). \tag{2.7}$$

In other words, v is approximated by 0.

Method 2: If we assume that the time derivative of the v part is small and we approximate it by 0, we arrive at a second type of method. This is the first type of nonlinear Galerkin methods studied in [6]:

$$\begin{array}{rcl} \frac{d\tilde{u}}{dt} & = & f(\tilde{u}, \tilde{v}, t) \\ 0 & = & g(\tilde{u}, \tilde{v}, t). \end{array} \tag{2.8}$$

Note that this requires that an implicit equation be solved and thus puts restrictions on g (see analysis below). In practice, iterative approximation solutions of $g(\tilde{u}, \tilde{v}, t) = 0$ are used.

Method 3: If, instead of assuming the first time derivative vanishes, we assume the second time derivative is zero, we arrive at a more developed nonlinear Galerkin method [6].

$$\begin{array}{rcl} \frac{d\tilde{u}}{dt} & = & f(\tilde{u}, \tilde{v}, t) \\ 0 & = & g_u(\tilde{u}, \tilde{v}, t) f(\tilde{u}, \tilde{v}, t) + g_v(\tilde{u}, \tilde{v}, t) g(\tilde{u}, \tilde{v}, t) + g_t(\tilde{u}, \tilde{v}, t). \end{array} \tag{2.9}$$

Method 4: In methods 2 and 3, we implicitly assume either the first or second time derivative of v to be small. This is not always the case, and is not assumed for this method:

$$\begin{array}{rcl} \frac{d\tilde{u}}{dt} & = & f(\tilde{u}, \tilde{v}, t) \\ \tilde{v} & = & \int^t e^{g_v(\tilde{u}, 0, t)(t-\tau)} g(\tilde{u}, 0, t) d\tau. \end{array} \tag{2.10}$$

The model reduction corresponds to assuming,

$$g(u, v, t) \approx g(u, 0, t) + g_v(u, 0, t) v. \tag{2.11}$$

Method 5: This method is used to recover the original y by postprocessing, and corresponds to solving the full system (2.6) for a few time steps at the end of the calculation. Giving

$$y \approx r(u, t).$$

See (2.4). This technique is studied in [7], [31].

These five methods are studied in more detail below.

2.3 Practical Implementation

Methods 2–4, when implemented directly, may be as computationally costly as solving the full system (2.6). Further simplifications are needed. For example, there is the issue of approximating the Jacobian g_v. Often in control theory, Padé approximations are used [27]. This makes for a straightforward, yet sometimes unstable, calculation. A Lanczos algorithm has been proposed [30] to fix the stability problems of the Padé approximation. Other approaches include matrix continued fraction approximations [24], optimization techniques [3], [17].

Another issue is the problem itself. Note that for Methods 2–4 the Jabobians should not become singular.

As an example consider (2.8) with linear f and g:

$$\begin{cases} \frac{d\tilde{u}}{dt} &= A\tilde{u} + B\tilde{v} + h_1 \\ 0 &= C\tilde{u} + D\tilde{v} + h_2. \end{cases}$$

Thus

$$\frac{d\tilde{u}}{dt} = (A\tilde{u} + BD^{-1}C)\tilde{u} + h_1 - BD^{-1}.$$

When $dim(\tilde{u}) \ll dim(\tilde{v})$ the full vector $\tilde{v}$ should not be solved for. Instead, some approximation of $BD^{-1}C$ must be implemented so D^{-1} is not computed.

2.4 Preliminary Error Analysis

How large errors will the methods of §2.2 produce? What follows is the preliminary steps towards a rigorous error analysis.

2.4.1 Overview

Preliminary error analysis of these methods is summarized in the following table:

Method	Order of Error
1	$\mathcal{O}(\|v\|)$
2–3	$\mathcal{O}(\|\frac{d^n}{dt^n}v\|)$
4	$\mathcal{O}(\|v\|^2)$

Table 1: Comparison of Error

The NLG vary in order, but are of the order of an nth derivative of v, for some n. Note that if the reduced variables v are small yet are changing rapidly, e.g., on transient phases, the new method is superior to the SGM and the NLG. There are conditions for these results to hold, specifically related to the Jacobians $\frac{\partial f}{\partial u}$, $\frac{\partial f}{\partial v}$, $\frac{\partial g}{\partial u}$, and $\frac{\partial g}{\partial v}$.

2.4.2 Method 1

Recall that we are approximating the full system, (2.1). Start with

$$\begin{cases} \frac{du}{dt} &= f(u,v,t) \\ \frac{d\tilde{u}}{dt} &= f(\tilde{u},0,t) \end{cases}$$

So

$$\begin{aligned} \tfrac{d(u-\tilde{u})}{dt} &= f(u,v,t) - f(\tilde{u},0,t) \\ &= f_u(u-\tilde{u}) + f_v v \end{aligned}$$

Let $Q_1 = f_u$.
Then

$$\begin{aligned} u - \tilde{u} &= \int^t f_v v \exp(\textstyle\int^{t-\tau} Q_1(s)ds)d\tau \\ \Rightarrow \|u-\tilde{u}\| &\leq \int^t \|f_v\|\|v\|\|\exp(\textstyle\int^{t-\tau} Q_1(s)ds)\|\tau \\ \Rightarrow \|u-\tilde{u}\| &\leq C_1 \textstyle\int^t q_1(t,\tau)d\tau\|v\| \end{aligned}$$

where $C_1 \geq \|f_v\|$ and $q_1(t,\tau) = \|\exp(\int^{t-\tau} Q_1(s)ds\|$.

At worst this gives the estimate:

$$\|u-\tilde{u}\| \leq \frac{C_1}{\|Q_1\|}(\exp(\|Q_1\|t) - 1)\|v\|.$$

There are cases where this can be improved. Specifically, if $\int^t q_1(t,\tau)d\tau < C_2$ then we have

$$\|u-\tilde{u}\| \leq C_1 C_2 \|v\|$$

where C_i are independent of t. One case this occurs is if $Q_1(t) \equiv Q_1$ and $\mathrm{Re}(\sigma(Q_1)) < 0$.

2.4.3 Method 2

Start with

$$\begin{cases} \frac{dv}{dt} &= g(u,v,t) \\ 0 &= g(\tilde{u},\tilde{v},t) \end{cases}$$

Then

$$\begin{aligned} \frac{dv}{dt} &= g(u,v,t) - g(\tilde{u},\tilde{v},t) \\ \Rightarrow \frac{dv}{dt} &= g_u(u-\tilde{u}) - g_v(v-\tilde{v}) \\ \Rightarrow v-\tilde{v} &= g_v^{-1}(\frac{dv}{dt} - g_u(u-\tilde{u})) \end{aligned}$$

Now

$$\begin{cases} \frac{du}{dt} &= f(u,v,t) \\ \frac{d\tilde{u}}{dt} &= f(\tilde{u},\tilde{v},t) \end{cases}$$

So

$$\begin{aligned} \frac{d(u-\tilde{u})}{dt} &= f(u,v,t) - f(\tilde{u},\tilde{v},t) \\ &= f_u(u-\tilde{u}) + f_v(v-\tilde{v}) \\ &= f_u(u-\tilde{u}) + f_v g_v^{-1}(\frac{dv}{dt} - g_u(u-\tilde{u})) \\ \frac{d(u-\tilde{u})}{dt} &= (f_u - f_v g_v^{-1} g_u)(u-\tilde{u}) + f_v g_v^{-1}\frac{dv}{dt} \end{aligned}$$

Let $Q_2 = f_u - f_v g_v^{-1} g_u$.
Then

$$\begin{aligned} u-\tilde{u} &= \int^t f_v g_v^{-1}\frac{dv}{dt}\exp(\textstyle\int^{t-\tau} Q_2(s)ds)d\tau \\ \Rightarrow \|u-\tilde{u}\| &\leq \int^t \|f_v g^{-1}\|\|\frac{dv}{dt}\|\|\exp(\textstyle\int^{t-\tau} Q_2(s)ds)\|\tau \\ \Rightarrow \|u-\tilde{u}\| &\leq C_1\int^t q_2(t,\tau)d\tau\|\frac{dv}{dt}\| \end{aligned}$$

where $C_3 \geq \|f_v g^{-1}\|$ and $q_2(t,\tau) = \|\exp(\int^{t-\tau} Q_2(s)ds)\|$.

At worst this gives the estimate:

$$\|u-\tilde{u}\| \leq \frac{C_3}{\|Q_2\|}(\exp(\|Q_2\|t)-1)\|\frac{dv}{dt}\|.$$

If $\int^t q_2(t,\tau)d\tau < C_4$ then we can improve the estimate to

$$\|u-\tilde{u}\| \leq C_3 C_4\|\frac{dv}{dt}\|$$

where C_i are independent of t. One case this occurs is if $Q_2(t) \equiv Q_2$ and $\mathrm{Re}(\sigma(Q_2)) < 0$.

2.4.4 Method 3

From the method, we start with

$$0 = g_u(\tilde{u},\tilde{v},t)f(\tilde{u},\tilde{v},t) + g_v(\tilde{u},\tilde{v},t)g(\tilde{u},\tilde{v},t) + g_t(\tilde{u},\tilde{v},t).$$

By differentiating the original equation, we get

$$\begin{aligned}
\tfrac{d^2v}{dt^2} &= \tfrac{d}{dt}(g(u,v,t)) \\
&= g_u(u,v,t)\tfrac{du}{dt} + g_v(u,v,t)\tfrac{dv}{dt} + g_t(u,v,t) \\
&= g_u(u,v,t)f(u,v,t) + g_v(u,v,t)g(u,v,t) + g_t(u,v,t)\cdots \\
&\quad -g_u(\tilde{u},\tilde{v},t)f(\tilde{u},\tilde{v},t) + g_v(\tilde{u},\tilde{v},t)g(\tilde{u},\tilde{v},t) + g_t(\tilde{u},\tilde{v},t)).
\end{aligned}$$

Upon subtracting,

$$\begin{aligned}
\tfrac{d^2v}{dt^2} &= h_u^1(u-\tilde{u}) + h_v^1(v-\tilde{v}) + h_u^2(u-\tilde{u}) + h_v^2(v-\tilde{v})\cdots \\
&\quad +g_{tu}(u-\tilde{u}) + g_{tv}(v-\tilde{v})
\end{aligned}$$

where $g_u(u,v,t)f(u,v,t) = h^1(u,v,t)$, and $g_v(u,v,t)g(u,v,t) = h^2(u,v,t)$.

Then

$$\begin{aligned}
v-\tilde{v} &= (g_{tu} + h_v^1 + h_v^2)^{-1}(\tfrac{d^2v}{dt^2} - (g_{tu} + h_u^1 + h_u^2)(u-\tilde{u})) \\
&= S_1\tfrac{d^2v}{dt^2} - S_2(u-\tilde{u}).
\end{aligned}$$

where $S_1 = (g_{tu} + h_v^1 + h_v^2)^{-1}$ and $S_2 = (g_{tu} + h_v^1 + h_v^2)^{-1}(g_{tu} + h_u^1 + h_u^2)$.

Now

$$\begin{cases} \frac{du}{dt} = f(u,v,t) \\ \frac{d\tilde{u}}{dt} = f(\tilde{u},\tilde{v},t) \end{cases}$$

So

$$\begin{aligned}
\tfrac{d(u-\tilde{u})}{dt} &= f(u,v,t) - f(\tilde{u},\tilde{v},t) \\
&= f_u(u-\tilde{u}) + f_v(v-\tilde{v}) \\
&= f_u(u-\tilde{u}) + f_v(S_1\tfrac{d^2v}{dt^2} - S_2(u-\tilde{u})) \\
\tfrac{d(u-\tilde{u})}{dt} &= (f_u - f_vS_2)(u-\tilde{u}) + f_vS_1\tfrac{d^2v}{dt^2}
\end{aligned}$$

Let $Q_3 = f_u - f_vS_2$.

Then

$$\begin{aligned}
u-\tilde{u} &= \int^t f_vS_1\tfrac{d^2v}{dt^2}\exp(\textstyle\int^{t-\tau} Q_3(s)ds)d\tau \\
\Rightarrow \|u-\tilde{u}\| &\le \textstyle\int^t \|f_vS_1\|\|\tfrac{d^2v}{dt^2}\|\|\exp(\int^{t-\tau} Q_3(s)ds)\|\tau \\
\Rightarrow \|u-\tilde{u}\| &\le C_3\textstyle\int^t q_3(t,\tau)d\tau\|\tfrac{dv}{dt}\|
\end{aligned}$$

where $C_5 \geq \|f_v S_1\|$ and $q_3(t,\tau) = \|\exp(\int^{t-\tau} Q_3(s)ds)\|$.

At worst this gives the estimate:

$$\|u - \tilde{u}\| \leq \frac{C_5}{\|Q_3\|}(\exp(\|Q_3\|t) - 1)\|\frac{d^2v}{dt^2}\|.$$

There are, however, cases where this error can be improved. Specifically, if $\int^t q_3(t,\tau)d\tau < C_6$ then we have

$$\|u - \tilde{u}\| \leq C_5 C_6 \|\frac{d^2v}{dt^2}\|$$

where C_i are independent of t. One case this occurs is if $Q_3(t) \equiv Q_3$ and $\mathrm{Re}(\sigma(Q_3)) < 0$.

2.4.5 Method 4

Start with

$$\begin{cases} \frac{dv}{dt} &= g(u,v,t) \\ \frac{d\tilde{v}}{dt} &= g(\tilde{u},0,t) + g_v(\tilde{u},0,t)\tilde{v} \end{cases}$$

So

$$\begin{aligned} \frac{d(v-\tilde{v})}{dt} &= g_u(u_1,v_1,t)(u-\tilde{u}) + g_v(\tilde{u},0,t)\tilde{v} \\ &= g_u(u_1,v_1,t)(u-\tilde{u}) + g_v(u_2,v_2,t)v + g_v(\tilde{u},0,t)(v-\tilde{v}) - g_v(\tilde{u},0,t)v \\ &= g_v(\tilde{u},0,t)(v-\tilde{v}) + g_u(u_1,v_1,t)(u-\tilde{u}) + (g_v(u_2,v_2,t) - g_v(\tilde{u},0,t))v \end{aligned}$$

Let

$$\begin{aligned} W_1 &= g_v(u_2,v_2,t) - g_v(\tilde{u},0,t) \\ &= g_{vu}(u_3,v_3,t)(u_2-\tilde{u}) + g_{vv}(u_4,v_4,t)v \end{aligned}$$

Note that since $\|u_2 - \tilde{u}\| \leq \|u - \tilde{u}\|$, $\|W_1\| \leq \|g_{vu}\|\|u-\tilde{u}\| + \|g_{vv}\|\|v\|$.

Solving the linear differential equation for $v - \tilde{v}$ gives:

$$v - \tilde{v} = \int^t (g_u(u-\tilde{u}) + W_1 v)\exp(\int^{t-\tau} g_v ds)d\tau$$

From the equations for u and $\tilde{u}$, we get

$$\begin{aligned} \frac{d(u-\tilde{u})}{dt} &= f_u(u-\tilde{u}) + f_v(v-\tilde{v}) \\ &= f_u(u-\tilde{u}) + f_v(\int^t (g_u(u-\tilde{u}) + W_1 v)\exp(\int^{t-\tau} g_v ds)d\tau) \\ &= f_u(u-\tilde{u}) + W_2, \end{aligned}$$

where $W_2 = f_v(\int^t (g_u(u-\tilde{u}) + W_1 v)\exp(\int^{t-\tau} g_v ds)d\tau)$. Solving this d.e. for $u-\tilde{u}$ gives

$$\begin{array}{rcl} u-\tilde{u} & = & \int^t W_2 \exp(\int^{t-\tau} f_u ds)d\tau \\ \Rightarrow \|u-\tilde{u}\| & \leq & \|W_2\| I_1(t). \end{array}$$

where $I_1(t) = \int^t \exp(\int^{t-\tau} f_u ds)d\tau$.

At this point care must be taken as to the estimate of $\|W_2\|$.

Note

$$\begin{array}{rcl} \|W_2\| & \leq & \|f_v\|(\int^t (\|g_u\|\|u-\tilde{u}\| + \|W_1\|\|v\|)\| \exp(\int^{t-\tau} g_v ds)\|d\tau \\ & \leq & \|f_v\|(\|g_u\|\|u-\tilde{u}\| + \|W_1\|\|v\|)I_2(t), \end{array}$$

where $I_2(t) = \int^t \exp(\int^{t-\tau} g_v ds)d\tau$. Using the estimate for W_1, the inequality becomes

$$\begin{array}{rcl} \|W_2\| & \leq & I_2(t)\|f_v\| \left(\|g_u\|\|u-\tilde{u}\| + (\|g_{vu}\|\|u-\tilde{u}\| + \|g_{vv}\|\|v\|)\|v\|\right) \\ & \leq & I_2(t)\|f_v\| \left((\|g_u\| + \|g_{vu}\|\|v\|)\|u-\tilde{u}\| + \|g_{vv}\|\|v\|^2\right). \end{array}$$

We now obtain an estimate for $u-\tilde{u}$:

$$\begin{array}{rcl} \|u-\tilde{u}\| & \leq & \|W_2\| I_1(t) \\ & \leq & I_1(t)\left(I_2(t)\|f_v\|(\|g_u\| + \|g_{vu}\|\|v\|)\|u-\tilde{u}\| + \|g_{vv}\|\|v\|^2)\right) \end{array}$$

$$\Rightarrow \|u-\tilde{u}\|(1 - I_1(t)I_2(t)\|f_v\|(\|g_u\| + \|g_{vu}\|\|v\|)) \leq I_1(t)I_2(t)\|f_v\|\|g_{vv}\|\|v\|^2$$

Let $D_1 = 1 - I_1(t)I_2(t)\|f_v\|(\|g_u\| + \|g_{vu}\|\|v\|) = o(1)$ as $\|v\| \to 0$.

Thus we must require

$$\begin{array}{rcl} 0 & < & D_1 \\ \Leftrightarrow 0 & < & 1 - I_1(t)I_2(t)\|f_v\|(\|g_u\| + \|g_{vu}\|\|v\|) \\ \Rightarrow 1 & > & I_1(t)I_2(t)\|f_v\|(\|g_u\| + \|g_{vu}\|\|v\|) \end{array}$$

Coarse estimates for I_1 and I_2 are

$$I_1(t) \leq \frac{1}{\|f_u\|}(\exp(\|f_u\|t) - 1)$$

$$I_2(t) \leq \frac{1}{\|g_v\|}(\exp(\|g_v\|t) - 1).$$

Then we can give a more restrictive estimate:

$$\|f_u\|\|g_v\| > (\exp(\|g_v\|t) - 1)(\exp(\|f_v\|t) - 1)\|f_v\|(\|g_u\| + \|g_{vu}\|\|v\|)$$

If this holds we have an estimate for $u - \tilde{u}$

$$\|u - \tilde{u}\| \leq \frac{1}{D_1} I_1(t) I_2(t) \|f_v\| \|g_{vv}\| \|v\|^2.$$

There are cases where this can be improved. Specifically, if $I_1(t) < C$ and $I_2(t) < C'$, and $\|f_v\|, \|g_{vv}\|$ are bounded and D_1 is bounded away from zero, then we have

$$\|u - \tilde{u}\| \leq Const \|v\|^2$$

independent of t. One case this occurs is if $f_u(t) \equiv f_u$, $g_v(t) \equiv g_v$, $\mathrm{Re}(\sigma(f_u)) < 0$, and $\mathrm{Re}(\sigma(g_v)) < 0$.

3 Applications

In this section two sets of numerical experiments are presented. The first is a pair of ODE's with some interesting properties. The second is the Burgers' equation. Analysis of the results follow.

3.1 Two simple ODE's

We begin by considering the following model ODE system:

$$\frac{du}{dt} + A_1(u) + R_1(u, v) = f_1(t) \tag{3.1}$$

$$\frac{dv}{dt} + A_2(v) + R_2(u, v) = f_2(t) \tag{3.2}$$

where A_1 and A_2 are linear operators, R_1 and R_2 are nonlinear functions. We assume A_2 has a larger positive real part than A_1.

Here the methods from §2 are presented for this setting and a group of numerical experiments explained.

3.1.1 Methods

The methods 1 through 4 can be posed as follows: Solve the following system.

$$\frac{d\tilde{u}}{dt} + A_1(\tilde{u}) + R_1(\tilde{u}, \Phi_{app}(\tilde{u})) = f_1(t) \tag{3.3}$$

where $\tilde{v} = \Phi_{app}(\tilde{u}) \approx v$. Hence to distinguish the Φ_{app} is to distinguish the method.

Method 1: The first try at this is to project onto u, i.e., we set $\Phi_0(u) = 0 \approx v$ and then time integrate (3.3).

Method 2a: Recall the assumption that

$$\frac{d\tilde{v}}{dt} = 0.$$

Then we can set

$$\begin{aligned} \tilde{v} &= A_2^{-1}(f_2(t) - R_2(\tilde{u}, 0)). \\ \Phi_1(\tilde{u}) &= \tilde{v}, \end{aligned}$$

and time integrate (3.3). Note Φ_1 is merely one fixed point iteration. It is also equivalent to the first nonlinear Galerkin method (Φ_1 in [19]).

Method 2b: Do the same as above except solve:

$$\begin{aligned} \tilde{v}_1 &= A_2^{-1}(f_2(t) - R_2(\tilde{u}, 0)). \\ \tilde{v}_2 &= A_2^{-1}(f_2(t) - R_2(\tilde{u}, \tilde{v}_1)) \\ \Phi_2(\tilde{u}) &= \tilde{v}_2, \end{aligned}$$

then time integrate (3.3). This is merely two fixed point iterations. and is equivalent to the second in a class of nonlinear Galerkin method studied in [6] (Φ_2).

Method 3: This method varies from the previous two methods in that it attempts to adjust the assumption that $\frac{dv}{dt} \approx 0$. To derive this method, take the time derivative of (3.2), then,

$$\frac{d^2v}{dt^2} + A_2(\frac{dv}{dt}) + \frac{\partial R_2(u,v)}{\partial u}\frac{du}{dt} + \frac{\partial R_2(u,v)}{\partial v}\frac{dv}{dt} = f_2'(t). \qquad (3.4)$$

Now approximate (3.4) by setting $\frac{d^2\tilde{v}}{dt^2} = 0$ and solving for $\tilde{v}^1$, the approximate time derivative:

$$A_2(\tilde{v}^1) + \frac{\partial R_2(\tilde{u}, \Phi_2(\tilde{u}))}{\partial u}(f_1(t) - A_1(\tilde{u}) - R_1(\tilde{u}, \Phi_2(\tilde{u}))) = f_2'(t). \quad (3.5)$$

Then set

$$\begin{aligned} \tilde{v}_3 &= A_2^{-1}(f_2(t) - R_2(u, \Phi_2(\tilde{u})) - \tilde{v}^1) \\ \Phi_3(\tilde{u}) &= \tilde{u}_3, \end{aligned}$$

and solve $\tilde{u}$ by integrating (3.3). This is similar to the nonlinear Galerkin method outlined in [7].

Method 4: In this new method, we avoid assuming that v or one of its time derivatives is 0. To do this we linearize as in (3.2), and then solve the resulting linear differential equation exactly, i.e,

$$\begin{aligned} \tilde{v} &= \frac{f_2(t)-R_2(\tilde{u},0,t)}{A_2+\frac{\partial R_2(\tilde{u},0,t)}{\partial u}}(1-\exp(-(A_2+\frac{\partial R_2(\tilde{u},0,t)}{\partial u})\Delta t)) \\ \Phi_4(\tilde{u}) &= \tilde{v}. \end{aligned} \tag{3.6}$$

Then solve for $\tilde{u}$ by integrating (3.3)

$$\frac{d\tilde{u}}{dt} + A_1(\tilde{u}) + R_1(\tilde{u}, \Phi_4(\tilde{u})) = f_1(t). \tag{3.7}$$

Method 5: In this method, we postprocess using Φ_2:

1. Calculate using Method 1 for all but the last few time steps.
2. Use Φ_2 for the last few Runge-Kutta steps.

In this method we attempt to recover (see (2.4)) the whole system after projecting for most of the time. This type of method was studied is [10].

3.1.2 Numerical Experiments

For the first numerical experiments, u and v were scalars, and the following system was considered.

$$\begin{aligned} \frac{du}{dt} + u + \sin(2\pi(u+v)) &= \frac{1}{4}(\sin(\mu t)+1), \\ \frac{dv}{dt} + 5v + \cos(u+v) &= 1, \\ u(0) &= 3, \\ v(0) &= 1, \end{aligned}$$

This system has some important properties. First, there are two variables with different decay rates: u is the slow part, v is the fast part. Secondly, in the evolution of the equations, there are two distinct stages: a transient stage at the beginning where the variables decay, and a stable long-time stage. The

period of the long-time stage was adjusted by varying μ. The results for cases $\mu = \pi$ and $\mu = 2\pi$ are reported.

Also note that the "Jacobian" g_v is never singular since $|5-\sin(u+v)| > 0$.

Fourth order Runge-Kutta with a step size of $k = 0.01$ was used for all time integrations.

It is important to note the performance of the different methods versus the fully computed solution. Quantitatively, four cases are considered. First, the L^1 error for the whole time interval $0 \leq t \leq 7$. Next, the L^1 error on the transient stage time interval $0 \leq t \leq 2$. Also, L^1 error on the stable stage time interval $5 \leq t \leq 7$. Finally the error of the last value is computed. This is to see how well Method 5 works in recovering as in (2.4).

Tables 2 through 5 display the error for u for the case $\mu = \pi$. Table 2 shows the L^1-norm of the error for the whole time interval. Table 3 shows the L^1-norm of the error for the transient stage time interval. Table 4 does the same for the stable stage time interval. Table 5 shows the error of the last value.

Method	Error
1	7.56×10^{-2}
2a	2.03×10^{-2}
2b	1.23×10^{-2}
3	1.29×10^{-2}
4	7.24×10^{-3}

Table 2: L^1 Errors: $\mu = \pi$, $0 \leq t \leq 7$

Method	Error
1	1.03×10^{-1}
2a	4.67×10^{-2}
2b	3.58×10^{-2}
3	4.02×10^{-2}
4	1.93×10^{-2}

Table 3: L^1 Errors: $\mu = \pi$, $0 \leq t \leq 2$

Method	Error
1	6.30×10^{-2}
2a	8.62×10^{-3}
2b	1.95×10^{-3}
3	9.40×10^{-4}
4	1.67×10^{-3}

Table 4: L^1 Errors: $\mu = \pi$, $5 \leq t \leq 7$

Method	Error
1	6.81×10^{-2}
2a	1.01×10^{-2}
2b	2.20×10^{-3}
3	1.82×10^{-4}
4	1.00×10^{-3}
5 (w/2b)	3.27×10^{-2}

Table 5: Last Value Errors: $\mu = \pi$

Observe that, overall, Method 4 performed better than the other methods. Note especially that Method 4 performed better that the other methods on the transient phase. And, as the error analysis indicates, the Methods 2a through 3 are superior in accuracy on the steady phase.

The following figures graphically display the difference in the methods. Figures 1 through 9 plot the case $\mu = \pi$. Figure 1 plots u as computed using the Method 1 and u for the full system. Figure 2 does the same for Method 2a. Figure 3 plots v as computed for Method 2a and v for the full system. Figures 4–9 alternately plot u and v for Methods 2b–4.

All programs were run using the MATLAB programming environment on Sun-OS machines.

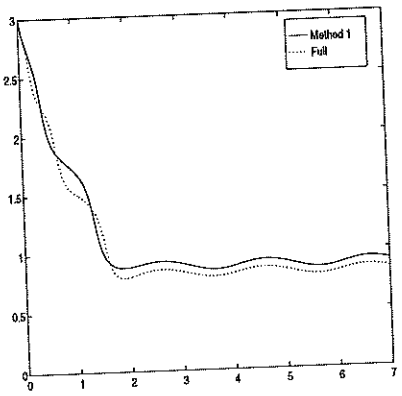

Figure 1: Method 1, u, $\mu = \pi$

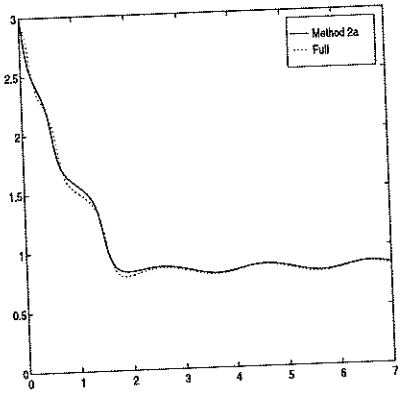

Figure 2: Method 2a, u, $\mu = \pi$

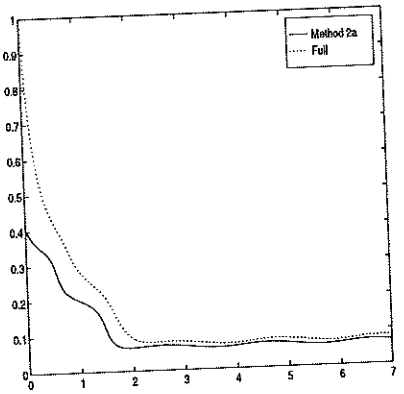

Figure 3: Method 2a, v, $\mu = \pi$

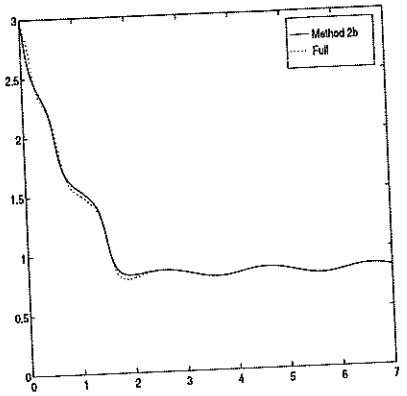

Figure 4: Method 2b, u, $\mu = \pi$

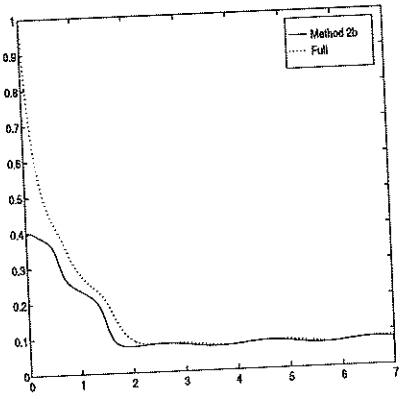

Figure 5: Method 2b, v, $\mu = \pi$

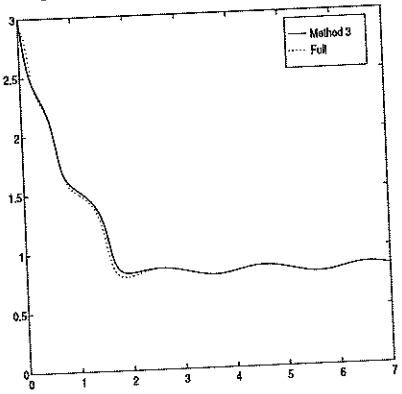

Figure 6: Method 3, u, $\mu = \pi$

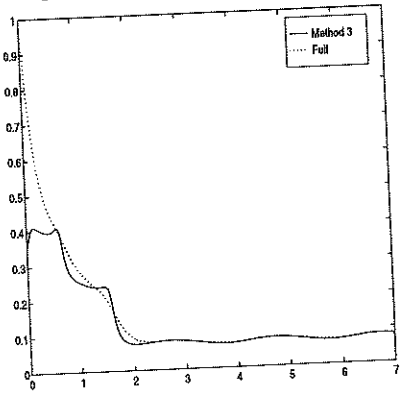

Figure 7: Method 3, v, $\mu = \pi$

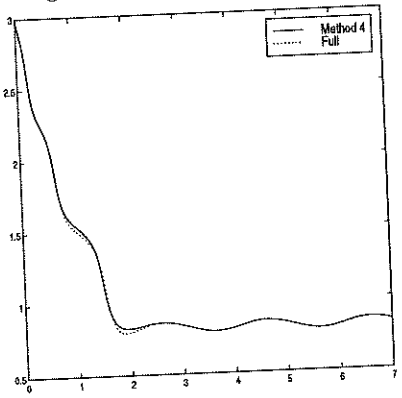

Figure 8: Method 4, u, $\mu = \pi$

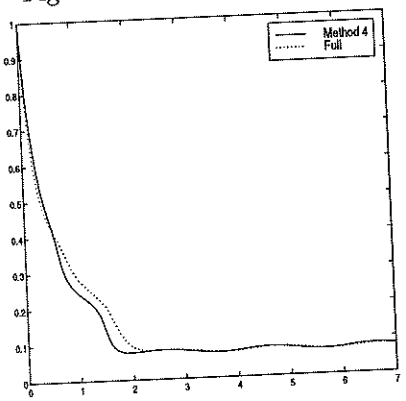

Figure 9: Method 4, v, $\mu = \pi$

3.2 1-D Burgers' Equation

The second set of experiments deal with Burgers' equation:

$$y_t + yy_x = \epsilon y_{xx} + f. \tag{3.8}$$

This can be written as a infinite dimensional abstract differential equation in $H = L^2([0, 2\pi])$.

$$\begin{aligned} \frac{d}{dt}y + \epsilon Ay + B(y) &= f \\ y(0) &= y_0, \end{aligned}$$

where A is the operator associated with $-\partial_{xx}$ and B is a bilinear operator that contains the nonlinear term.

We will consider as a basis, the usual Fourier modes, $w_j = e^{2\pi ijx}$, i.e., we use the Fourier spectral method.

The standard Galerkin method (SGM) calculates the solution on a fixed subspace of H, namely $H_m = span\{w_j\}, j = 1, \ldots, m$. Let P_m denote projection onto H_m, and $u_m = P_m(y)$. Then the SGM solves:

$$\begin{aligned} \frac{d}{dt}u_m + \epsilon Au_m + P_m(B(u_m, u_m)) &= P_m(f) \\ u_m(0) &= P_m(y(0)). \end{aligned}$$

Recent developments have arisen [19] that improve on this projection in a similar way as was done with the ODE's. The idea behind these so-called nonlinear Galerkin methods (NLG's) is to consider also the orthogonal compliment of H_m, and use the existence of the inertial manifold to approximate the part of the solution that lives there.

Let $Q_m = Iden - P_m$, and $v_m = Q_m(y)$. Then $H = P_m(H) \oplus Q_m(H)$, $y = u_m + v_m$, and (3.9) becomes:

$$\begin{aligned} \tfrac{d}{dt}u_m + \epsilon Au_m + P_m(B(y)) &= P_m(f) \\ \tfrac{d}{dt}v_m + \epsilon Av_m + Q_m(B(y)) &= Q_m(f), \end{aligned} \tag{3.9}$$

where $u_m = P_m(y)$ and $v_m = Q_m(y)$.

In practice, since H has infinite dimension, $Q_m = P_{Nm} - Q_m$, where N is a positive integer (e.g., 2).

Because the equation admits an inertial manifold [5], this system can be reduced. Specifically, there exists some smooth Φ such that, for solutions $y =$

$u_m + v_m$, we have $v_m = \Phi(u_m)$. In this notation, the inertial manifold $M = graph(\Phi)$. In general, this Φ is impossible to compute, so we approximate it. See [6], [14], [19], and references for many approximations. Let Φ_{app} denote the approximation to Φ.

The nonlinear Galerkin methods use this feature to compute the reduced solution similar to the standard Galerkin method, but more accurately, by solving the ordinary differential system:

$$\begin{aligned} \frac{d}{dt}u_m + \epsilon A u_m + P_m(B(u_m + \Phi_{app}(u_m))) &= P_m(f) \\ u_m(0) &= P_m(y(0)). \end{aligned}$$

3.2.1 Methods

We apply methods that are analogs of those in §2, using the Φ_{app} notation.

Methods 1–4 are distinguished only by their associated Φ_{app}. The following Φ_{app} were implemented:

Method 1: SGM with $\Phi_{app} = 0$ (see (2.8)).

Method 2a: Nonlinear Galerkin method 1 (NLG1) with $\Phi_{app} = \Phi_1$, in [6] (see (2.8)):

$$\Phi_1(u_m) = (\epsilon A)^{-1}(Q_m(f - B(u_m))).$$

Method 2b: Nonlinear Galerkin method 2 (NLG2) with $\Phi_{app} = \Phi_2$, in [6]: (see (2.8)):

$$\Phi_2(u_m) = (\epsilon A)^{-1}(Q_m(f - B(u_m + \Phi_1(u_m)))).$$

Method 3: Nonlinear Galerkin method 3 (NLG3) with $\Phi_{app} = \Phi_3$, in [6] (see (2.9)):

$$\Phi_3(u_m) = (\epsilon A)^{-1}(Q_m(f - B(u_m + v_{m,3})))$$

where $v_{m,3}$ is given by:

$$\begin{aligned} v_{m,2} &= \Phi_2(u_m) \\ u^1_{m,0} + \epsilon A u_m + P_m(B(u_m + v_{m,2})) &= P_m(f) \\ \epsilon A v^1_{m,2} + Q_m(B(u^1_{m,0}, u_m + v_{m,2}) + B(u_m + v_{m,2}, u^1_{m,0})) &= 0 \\ v^1_{m,2} + \epsilon A v_{m,3} + Q_m(B(u_m + v_{m,2})) &= Q_m(f) \end{aligned}$$

Method 4: New method with $\Phi_{app} = \Phi_4$ in (3.6):

$$\Phi_4(u_m) = (Q_m(\epsilon A + B_u(u_m)))^{-1} Q_m(B(u_m))(I - \exp(-(\epsilon A - B_u(u_m))\Delta t)$$

Method 5: Postprocessed Galerkin method (PSGM) using Φ_2, see [10]:

1. Calculate using SGM for desired time steps.
2. Postprocess result, i.e., set $y_{app}(T) = u_m(T) + \Phi_2(u_m(T))$, where T is the maximum time.

3.2.2 Numerical Experiments

For the experiments, the following three sets of initial data were used:

$$\begin{aligned} y_1(x,0) &= \sin(x) \\ y_2(x,0) &= \begin{cases} 0 & \text{for } x \in [0, \pi/4) \\ 1 & \text{for } x \in [\pi/4, 5\pi/4] \\ 0 & \text{for } x \in [5\pi/4, 2\pi] \end{cases} \\ y_3(x,0) &= 1 + \sin(x) \end{aligned}$$

For y_1, a calculations were run until $T = 3$ with a time step of 10^{-4}, y_2 and y_3 with a maximum time of $T = 2$ and a time step of 10^{-4}. Fourth order Runge-Kutta used for all time integrations.

All programs were run using the MATLAB programming environment on Sun-OS machines.

Figure 10 plots the exact the solutions. Figures 11–14 show the results of four methods (1 SGM , 2a NLG2, 4, and 5 PSGM) for the three types of initial data using 32 nodes, together with the exact solution. Figure 15 shows the convergence rates for the methods for the initial value y_1. Note that Methods 1 and 5 are grouped separately as they have significantly slower convergence rates from the others. Note that Method 4 compares favorably with the nonlinear Galerkin methods.

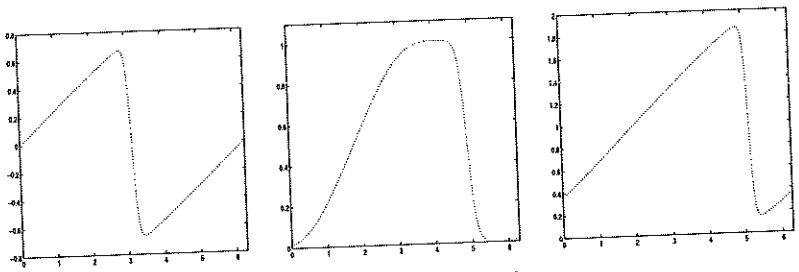

Figure 10: Exact Solutions

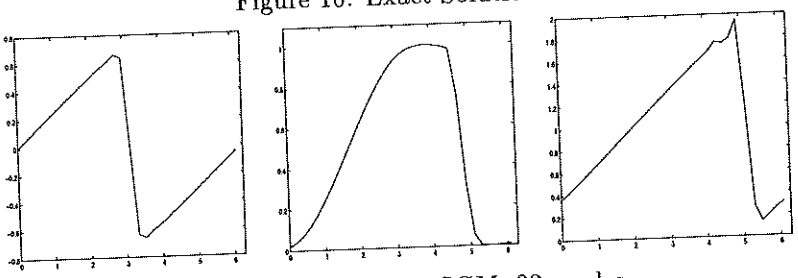

Figure 11: Method 1: SGM, 32 modes

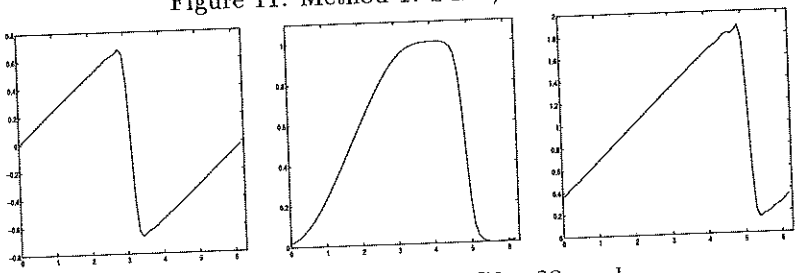

Figure 12: Method 2a: NLG2a, 32 modes

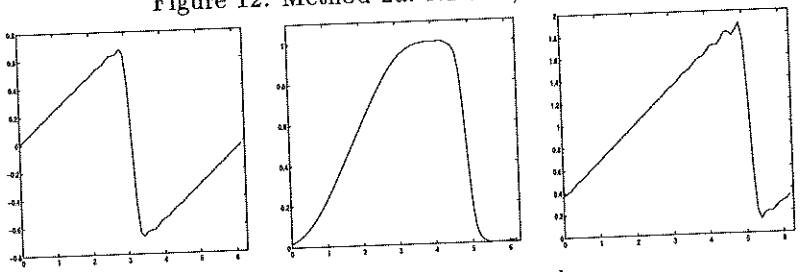

Figure 13: Method 4, 32 modes

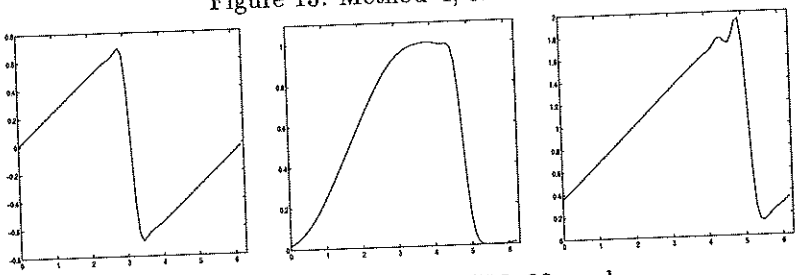

Figure 14: Method 5: PSGM, 32 modes

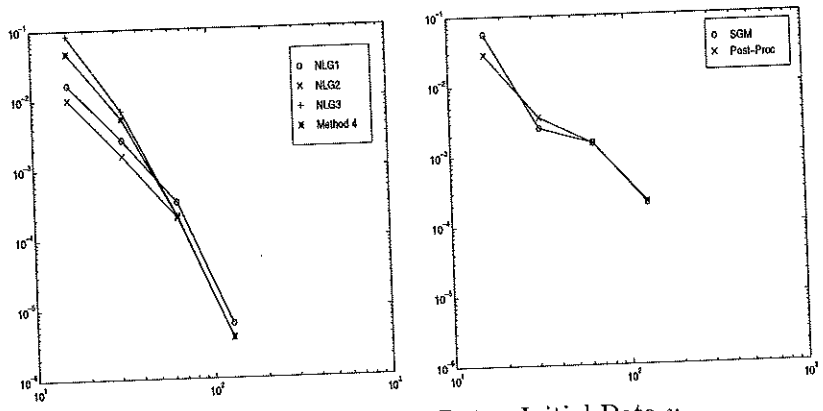

Figure 15: Convergence Rates, Initial Data y_1

3.3 Molecular Beam Epitaxy

In the control of molecular beam epitaxy (MBE) processes, it is important to have simple mathematical models. These models should describe the layer-by-layer growth of thin films on atomic scales. The growth can be represented by so-called island dynamics where an island consists of a compact monolayer.

At present the UCLA Mathematics Department is involved in a major MBE project. The full island dynamics model is a PDE model based on the motion of the boundaries of forming layers. The level set method was used for this model. This, however, is too computationally intense to implement control. Thus a reduced order model [2], based on the same physical quantities, is needed. Further along these same lines, model reduction is of interest.

The reduced-order model for single layer growth is as follows:

$$\begin{aligned} \tfrac{d}{dt}\{\psi + a^2\rho(1-\psi)\} &= a^2F(1-\psi) \\ \tfrac{d}{dt}\psi &= (fq+2m)a^2 \\ \tfrac{d}{dt}n &= m-c \end{aligned} \tag{3.10}$$

where

$$\begin{aligned}
\psi &= \text{island coverage} \\
\rho &= \text{adatom density} \\
q &= \text{step edge density} \\
f &= \text{flux to islands} \\
n &= \text{island number density} \\
m &= \text{island nucleation rate} \\
c &= \text{island coallescence rate.}
\end{aligned}$$

All the variables depend on ρ, n, and ψ explicitly (see the cited reference for details). The system can be algebraically transformed into the following form:

$$\begin{aligned}
\tfrac{d}{dt}\psi &= g_1(\psi, n, \rho) \\
\tfrac{d}{dt}n &= g_2(\psi, n, \rho) \\
\tfrac{d}{dt}\rho &= h(\psi, n, \rho).
\end{aligned} \tag{3.11}$$

Since the variable ρ remains small compared to ψ, and n, model reduction attempts begin with eliminating the evolution equation for ρ.

The model reduction methods can then be viewed as obtaining an approximation of ρ from the values of ψ and n.

$$\begin{aligned}
\tfrac{d}{dt}\tilde{\psi} &= g_1\left(\tilde{\psi}, \tilde{n}, \Phi_{app}(\tilde{\psi}, \tilde{n})\right) \\
\tfrac{d}{dt}\tilde{n} &= g_2\left(\tilde{\psi}, \tilde{n}, \Phi_{app}(\tilde{\psi}, \tilde{n})\right)
\end{aligned} \tag{3.12}$$

3.3.1 Methods

For this model just two of the methods were used, Method 2a and Method 4. Method 1 is unsuitable because, although ρ remains small for all time, it is the driving quantity for the start of the epitaxial growth, as the adatom density should be. So if its value is set to zero, the equations fail to model the system properly. Method 2b was not implemented since for this system, it is equivalent to 2a. Method 3 was not implemented because the resulting complexity of the system.

Method 2a:
For this method, simply resolve

$$0 = h(\psi, n, \tilde{\rho})$$

for $\tilde{\rho}$. This can be done with high accuracy as the resulting equation is simply a quadratic equation in ρ, giving $\Phi_2(\psi, n)$. (This is also the reason why Method 2b is equivalent.)

Method 4:
An approximation of the solution of

$$\frac{d}{dt}\tilde{\rho} = h(\tilde{\psi}, \tilde{n}, 0) + h_\rho(\tilde{\psi}, \tilde{n}, 0)\tilde{\rho}$$

is needed. Take

$$\begin{aligned} \tilde{\rho} &= (h_\rho(\psi, n, 0))^{-1} h(\psi, n, 0)(1 - e^{h_\rho(\psi,n,0)t} + e^{h_\rho(\psi,n,0)t}\rho_0 \\ \Phi_4(\psi, n) &= \tilde{\rho}. \end{aligned}$$

Note that this is a different approximation of the integral than was used previously.

3.3.2 Numerical Experiments

The methods were tested with values $a = 1$, $\rho_0 = 2 \times 10^{-6}$, $\psi_0 = \rho_0$, $n_0 = 10^{-6}$. Since the equations form a stiff system, a stiff solver was used: ODE15S in MATLAB for the full system and a standard algorithm (see [13]) for the others. Figures 17 - 19 show the fully computed solution and the reduced solutions, respectively. The quantity ρ is the approximated quantity. Note the superior approximation of Method 4 for this quantity, when compared with Method 2.

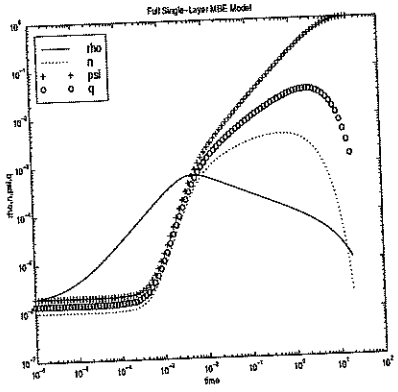

Figure 17: Fully computed solution

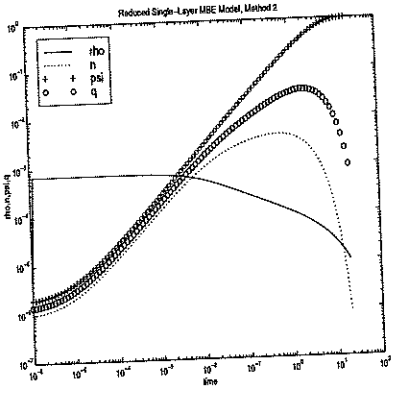

Figure 18: Reduced solution using Method 2

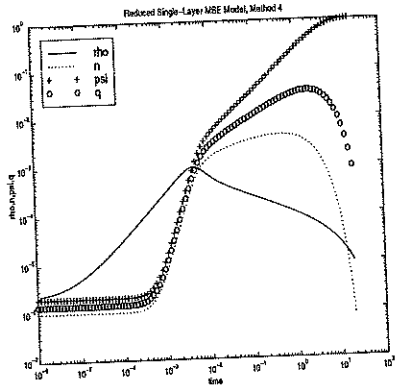

Figure 19: Reduced solution using Method 4

4 Conclusions

In conclusion, nonlinear Galerkin methods have been successfully cast in a general model reduction setting. Here a new method (Method 4) is derived in a similar way. The new method shows promise. The above analysis and applications demonstrate the usefulness of this reduction method, especially on the transient phases of a dynamical system. There is, however, the need for more research.

The effect of the reduction techniques on Burgers' equation must be studied more thoroughly. One approach may be to look at the effect of reducing more than one half of the modes. More rigorous error analysis must be done on the methods to give sharper error bounds, and determine when they are applicable. Work still needs to be done on efficient implementation of the methods. These technical issues will be addressed.

There is another interesting question that arises: What other uses does model reduction have? For instance, a full system of ODE's may be stiff, but after reduction, the stiff variables are eliminated. These more general questions will also be studied.

References

[1] U. Andersson, B. Engquist, G. Ledfelt, O. Runborg, A Contribution to Wavelet-Based Subgrid Modeling, *Preprint*, 1997.

[2] R. Caflisch, M. Gyure, D. Meyer, C. Ratsch, A Reduced Order Model for Epitaxial Growth, *Preprint*, 1998.

[3] R. Chiang and M. Safonov, Robust-control Toolbox, The MathWorks, South Natick, MA, 1988.

[4] M. Chen and R. Temam, Nonlinear Galerkin method in the finite difference and wavelet-like Incremental Unknowns, *Numer. Math*, **64**, 1993, 271-294.

[5] P. Constantin, C. Foias, B. Nicolaenko, R. Temam, *Integral Manifolds and Inertial Manifolds for Dissipative Partial Differential Equations*, Springer-Verlag, 1989.

[6] C. Devulder and M. Marion, A class of numerical algorithms for large time integration: the nonlinear Galerkin methods, *SIAM J. Numer. Anal.*, **29**, 1992, 462-483.

[7] C. Devulder, M. Marion, E. Titi, On the rate of convergence of the nonlnear Galerkin methods, *Math. Comp.*, **60**, 1993, 495-514.

[8] C. Foias, O. Manley, R. Temam, Iterated approximate inertial manifolds for the Navier-Stokes equations in 2-D, *J. Math. Anal Appl.*, **178**, 1993, 567-583.

[9] B. Garcia-Archilla, J. Novo, E. Titi, An Approximate Inertial Manifolds Approach to Postprocessing the Galerkin Method for the Navier-Stokes Equations, *Preprint*, 1996.

[10] B. Garcia-Archilla, J. Novo, E. Titi, Postprocessing the Galerkin method: a novel approach to the approximate inertial manifolds, *submitted to SIAM J. Numer. Anal.*, 1996.

[11] B. Gustafsson, H. Kreiss, J. Oliger, *Time Dependent Problems and Difference Methods*, John Wiley & Sons, 1995.

[12] K. Ito and S. Ravindran, Reduced Order Methods for Nonlinear Infinite Dimensional Control Systems, *Proceedings of the 36th Conference on Decision & Control*, 1997, 2213-2218.

[13] H. Hairer, G. Wanner, Solving Ordinary Differential Equations II, 2nd ed., Springer-Verlag, 1996.

[14] D. Jones, L. Margolin, E. Titi, On the effectiveness of the approximate inertial manifold–a computational study, *Theo. Comp. Fluid Dyn.*, **7**, 1995, 243-260.

[15] D. Jones and E. Titi, A Remark on Quasi-Stationary Approximate Inertial Manifolds for the Navier-Stokes Equations, *SIAM J. Math. Anal.*, **25**, 1994, 894-914.

[16] P. Kokotovic, R. O'Malley, P. Sannuti, Singular Perturbations and Order Reduction in Control Theory–An Overview, *Automatica*, **12**, 1976, 128-132.

[17] B. King and E. Sachs, Reduced Order Controllers for Partial Differential Equation Systems with Guaranteed Stability Margins, *Proceedings of the 36th Conference on Decision & Control*, 1997, 2219-2224.

[18] U. Maas, Efficient Calculation of Intrinsic Low-Dimensional Manifolds for Simplification of Chemical Kinetics, *Preprint*, 1997.

[19] M. Marion and R. Temam, Nonlinear Galerkin methods, *SIAM J. Numer. Anal.*, **26**, 1989, 1139-1157.

[20] M. Marion and R. Temam, Nonlinear Galerkin methods: the finite element case, *Numer. Math.*, **57**, 1990, 205-226.

[21] F. Mossayebi, T. Hartley, J. De Abreu-Garcia, A Fundamental Theorem for the Model Reduction of Nonlinear Systems, *J. Franklin Inst.*, **329**, 1992, 145-153.

[22] A. Noor, Recent Advances in Reduction Methods for Nonlinear Problems, *Computers & Structures*, **13**, 1981, 31-44.

[23] C. Foias, G.R. Sell, and R. Temam, Inertial manifolds for nonlinear evolutionary equations, *J. Diff. Eq.*, **73**, 1988, 309-353.

[24] B. Moore, Principal Component Analysis in Linear Systems: Controllability, Observability, and Model Reduction, *IEEE Trans. Auto. Control*, **AC-32**, 1981, 17-34.

[25] A. T. Norris, Application of Low Dimensional Manifolds in NOx Prediction, *NASA Contractor Report 204137*, 1997.

[26] A. T. Norris, Automated Simplification of Full Chemical Mechanisms, *NASA Contractor Report 204138*, 1997.

[27] Y. Shamash, Linear system reduction using Padé approximation to allow retention of dominant modes, *Int. J. Control*, **21**, 1975, 257-272.

[28] J. Shen and R. Temam, Nonlinear Galerkin methods using Chebyshev or Legendre polynomials I. One dimensional case, *SIAM J. Numer. Anal.* **32**, 1995, 215-234.

[29] L. Shieh and F. Gaudiang, Jr., Some Properities and Applications of Matrix Continued Fraction, *IEEE Trans. Circuits Systems*, **CAS-22**, 1975, 721-728.

[30] P. Van Dooren, Lanczos algorithm and Padé approximations, Lecture Notes, 1997?.

[31] J. Ystrom and H.-O. Kreiss, A Numerical Study of the Solution to the 3D Incompressible Navier-Stokes Equation with Forcing Function, UCLA CAM Report (98-31), 1998.